Supplemental material

Supplemental figure legends

Figure S1: Drosophila Rnf146/Iduna targets Tnks substrates for degradation *in vivo*.

(A-C) Third instar larval eye imaginal discs containing *Rnf146*^{36} null mutant clones marked by the absence of GFP (-/-; magenta) were stained with indicated antibodies. Proteins modified by poly-ADP-ribose accumulate cell autonomously in *Rnf146*^{36} mutant clones.

Figure S2: Drosophila Rnf146 mediates pADPr-directed destabilization of Axin and Tnks *in vivo*. (A) Immunoblot of lysates from wild-type and *Rnf146* null mutant embryos collected at indicated stages probed with Tnks or Axin antibody. Tnks and Axin protein levels are increased in *Rnf146* mutant embryos. Kinesin was used as a loading control. (B-D) Third instar larval eye imaginal discs containing *Rnf146*^{36} null mutant clones marked by the absence of GFP (-/-; magenta) were stained with indicated antibodies. Tnks accumulates cell autonomously in *Rnf146*^{36} null mutant clones.

Figure S3: An *in vivo* analysis of domains required for Tnks-dependent degradation of Axin.

Confocal images of third instar larval wing imaginal discs expressing indicated Axin-V5 transgenes with the *71B-Gal4* driver, which drives expression in the dorsal and ventral regions of the pouch of third instar larval wing imaginal discs. Axin mutants were stained with V5 antibody (green). *Tnks* mutant clones were marked by the lack of β-gal staining (magenta). The levels of AxinΔRGS (A-C) and AxinΔArm (D-F) increase in *Tnks* mutant clones compared with neighboring wild-type cells. The levels of AxinΔPP2A (G-L) and AxinΔDIX (M-R) increase in some, but not all cells within *Tnks* mutant clones compared with neighboring wild-type cells.

Figure S4: An *in vivo* analysis of domains required for Rnf146-dependent degradation of Axin.

Confocal images of third instar larval wing imaginal discs expressing indicated Axin transgenes with the *C765-Gal4* driver, which drives expression in the dorsal and ventral regions of the pouch of third instar larval wing imaginal discs. Axin mutants were stained with V5 antibody (green). *Rnf146* mutant clones were marked by the lack of GFP staining (magenta). The levels of AxinΔRGS (A-C) and AxinΔArm (D-F) increase in *Rnf146* mutant clones compared with neighboring wild-type cells. The levels of AxinΔPP2A (G-L) and AxinΔDIX (M-R) increase in some, but not all cells within *Rnf146* mutant clones compared with neighboring wild-type cells.

Figure S5: In contrast with Tnks, Rnf146 is dispensable for regulation of progenitor cell number in the adult midgut. Confocal images from midguts of 14 day old adults, genotypes indicated on top: $Tnks^{19/503}$ and $Rnf146^{36/157}$. Progenitor cells are marked by *esg-Gal4, UAS-GFP* (*esg-GFP*) stained with anti-GFP (green) and nuclei are marked with DAPI (blue). The difference in progenitor cell number between control (A) and *Rnf146* mutant midguts (B) is insignificant (Fig. 5), whereas the number of progenitor cells is increased in *Tnks* mutant midguts (C).

Figure S1

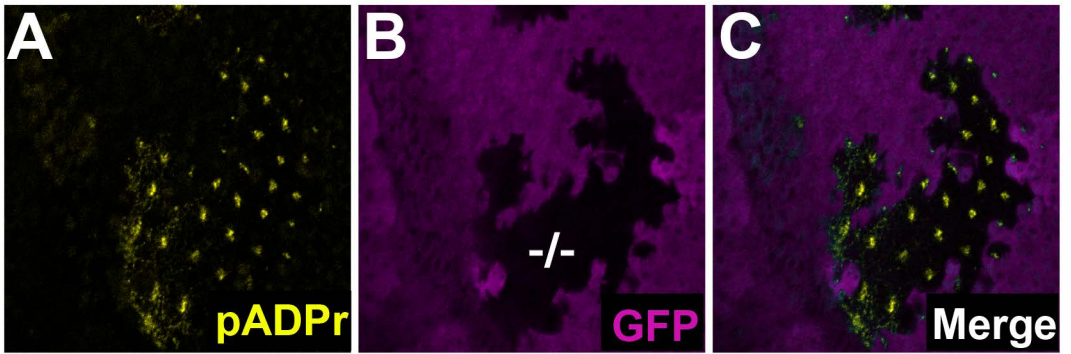

Figure S2

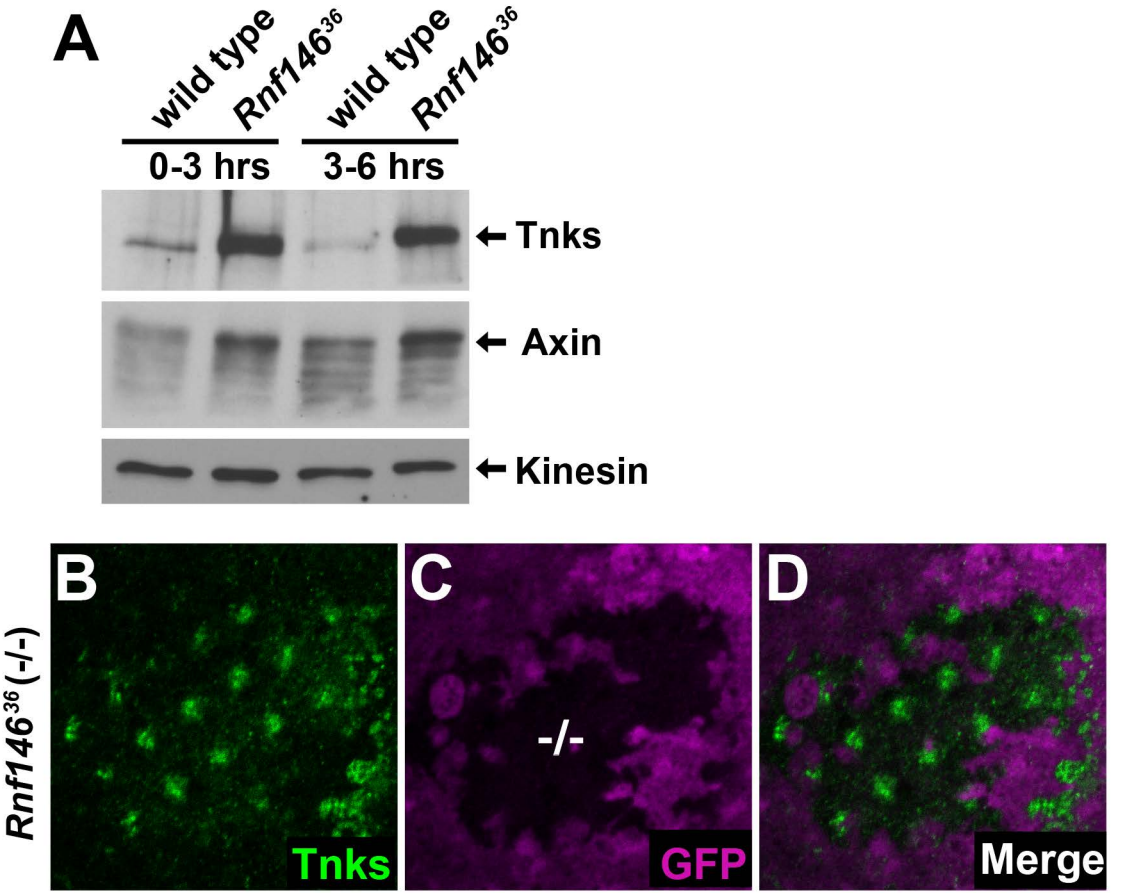
A
wild type
Rnf146^36
wild type
Rnf146^36
0-3 hrs
3-6 hrs
Tnks
Axin
Kinesin
B
C
D
Rnf146^36 (-/-)
Tnks
-/-
GFP
Merge

Figure S3

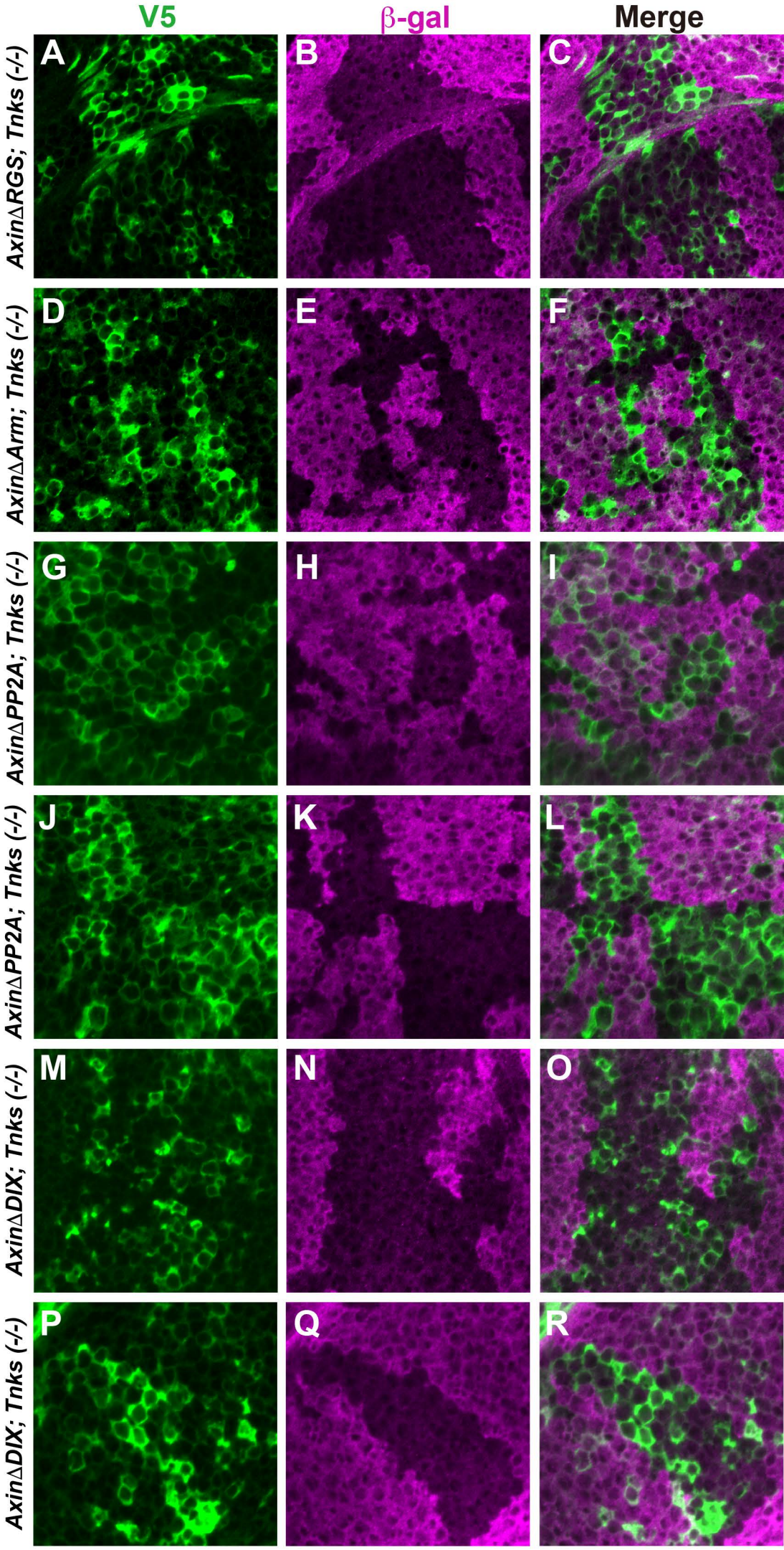
V5
β-gal
Merge
A
B
C
Axin∆RGS; Tnks (-/-)
D
E
F
Axin∆Arm; Tnks (-/-)
G
H
I
Axin∆PP2A; Tnks (-/-)
J
K
L
Axin∆PP2A; Tnks (-/-)
M
N
O
Axin∆DIX; Tnks (-/-)
P
Q
R
Axin∆DIX; Tnks (-/-)

Figure S4

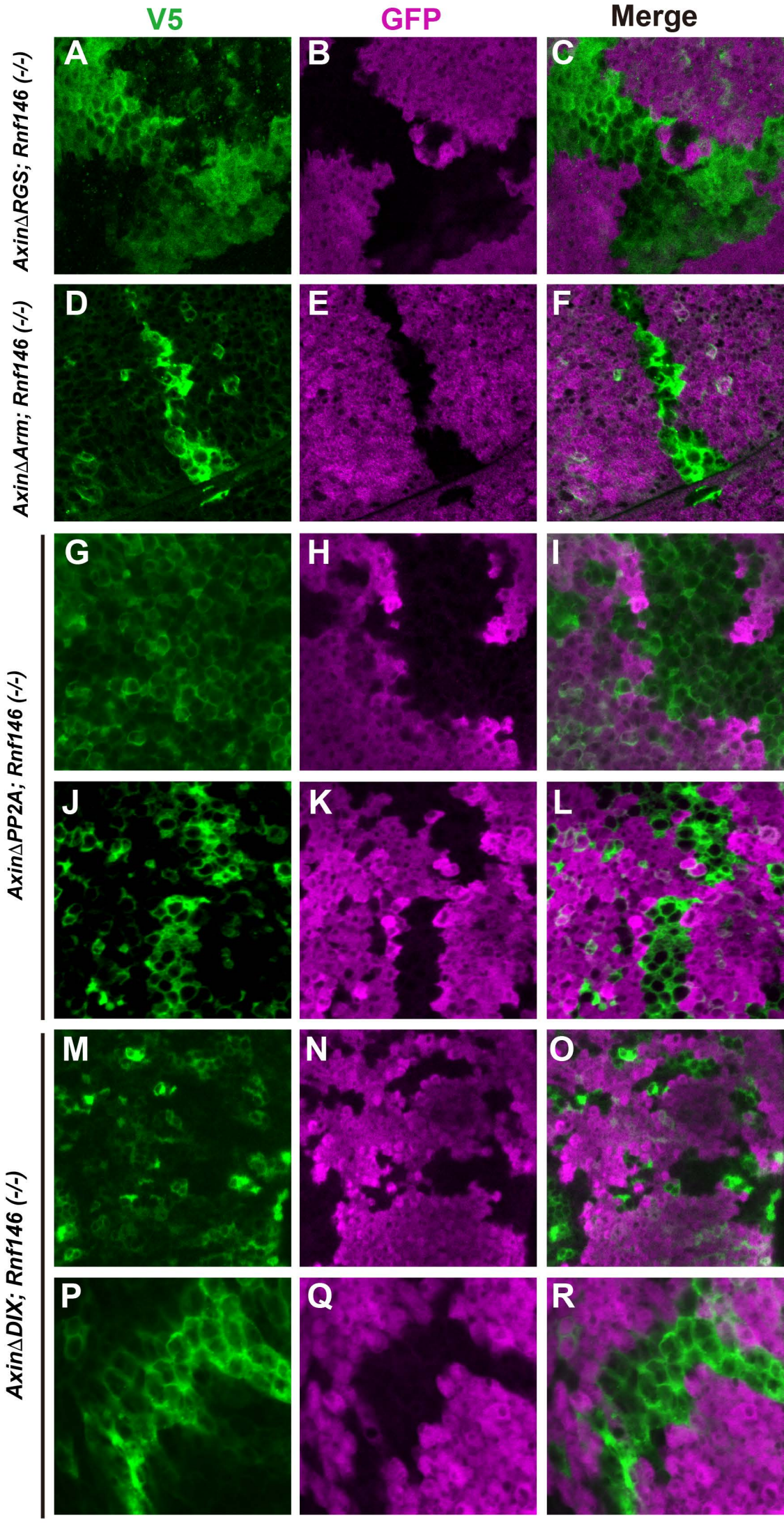
V5
GFP
Merge
A
B
C
Axin∆RGS; Rnf146 (-/-)
D
E
F
Axin∆Arm; Rnf146 (-/-)
G
H
I
J
K
L
Axin∆PP2A; Rnf146 (-/-)
M
N
O
P
Q
R
Axin∆DIX; Rnf146 (-/-)

Figure S5